Infrared Physics & Technology 89 (2018) 325–337

Contents lists available at ScienceDirect

Infrared Physics & Technology

journal homepage: www.elsevier.com/locate/infrared

Regular article

Automated characterization of diabetic foot using nonlinear features extracted from thermograms

Muhammad Adam [a,*], Eddie Y.K. Ng [b], Shu Lih Oh [a], Marabelle L. Heng [e], Yuki Hagiwara [a], Jen Hong Tan [a], Jasper W.K. Tong [f], U. Rajendra Acharya [a,c,d]

[a] Department of Electronics and Computer Engineering, Ngee Ann Polytechnic, Singapore
[b] School of Mechanical and Aerospace Engineering, Nanyang Technological University, Singapore
[c] Department of Biomedical Engineering, School of Science and Technology, SIM University, Singapore
[d] Department of Biomedical Engineering, Faculty of Engineering, University of Malaya, Malaysia
[e] Podiatry Department, Singapore General Hospital, Singapore
[f] Allied Health Office, KK Women's and Children's Hospital, Singapore

HIGHLIGHTS

- Characterization of diabetic foot is proposed using Infrared thermography.
- Nonlinear features extracted from thermograms.
- Ranked features are subjected to SVM classifier.
- Maximum accuracy of 89.39% using only *five* features.

GRAPHICAL ABSTRACT

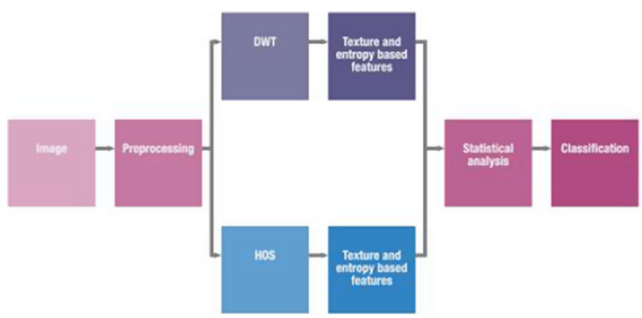

ARTICLE INFO

Article history:
Received 21 November 2017
Revised 17 January 2018
Accepted 17 January 2018
Available online 20 February 2018

Keywords:
Foot
Diabetes
Neuropathy
Plantar
Temperature
Infrared image

ABSTRACT

Diabetic foot is a major complication of diabetes mellitus (DM). The blood circulation to the foot decreases due to DM and hence, the temperature reduces in the plantar foot. Thermography is a non-invasive imaging method employed to view the thermal patterns using infrared (IR) camera. It allows qualitative and visual documentation of temperature fluctuation in vascular tissues. But it is difficult to diagnose these temperature changes manually. Thus, computer assisted diagnosis (CAD) system may help to accurately detect diabetic foot to prevent traumatic outcomes such as ulcerations and lower extremity amputation. In this study, plantar foot thermograms of 33 healthy persons and 33 individuals with type 2 diabetes are taken. These foot images are decomposed using discrete wavelet transform (DWT) and higher order spectra (HOS) techniques. Various texture and entropy features are extracted from the decomposed images. These combined (DWT + HOS) features are ranked using t-values and classified using support vector machine (SVM) classifier. Our proposed methodology achieved maximum accuracy of 89.39%, sensitivity of 81.81% and specificity of 96.97% using only *five* features. The performance of the proposed thermography-based CAD system can help the clinicians to take second opinion on their diagnosis of diabetic foot.

1. Introduction

Diabetes Mellitus (DM) is a progressive and chronic disorder due to either lack of insulin production by the pancreas or

* Corresponding author at: Department of Electronics and Computer Engineering, Ngee Ann Polytechnic, Singapore 599489, Singapore.
E-mail address: muhdadam@hotmail.com (M. Adam).

https://doi.org/10.1016/j.infrared.2018.01.022
1350-4495/

ineffective use of insulin by the body [1]. Over time, the high blood glucose levels may cause complications to the kidneys, heart, eyes, blood vessels and nerves [2]. An estimated 422 million people globally were living with diabetes in 2014 as compared to 108 million in 1980 [3]. The diabetic foot is a serious diabetes complication characterized by bacterial infection, foot ulceration, and deep tissues destruction which may be due to neuropathy and arterial disease in the lower limb [4]. The inability to sustain the stress makes diabetic foot significantly vulnerable to various foot complications that may lead to limb amputation. Diabetic foot ulcers (DFUs) complication critically affect around 15% of the diabetic population [5]. Moreover, diabetic patients are having 12–25% lifetime risk of developing foot ulcers [6] and almost 85% of the lower limb amputations are due to non-healing foot ulcers [7].

Diabetic foot complications can be prevented by early detection and proper clinical treatment. Based on International Working Group on the Diabetic Foot (IWGDF) risk category [8], diabetic patients need to screen their feet at least once every year to detect foot at risk of ulceration. The feet examination comprised of medical history and foot examination and, neuropathy assessment [8]. The medical history and foot examinations include previous history of amputation or ulceration and, health status of the vascular, skin, joint and bone [8]. Subsequently, neuropathy is assessed by performing these methods: enquiring on tingling or pain signs in the lower extremity; vibration perception using 128 Hz tuning fork; pressure perception using Semmes-Weinstein monofilaments; tactile sensation using cotton wool or by lightly touching the toes tips with index fingers; discrimination using pin prick on dorsum of foot superficial; and assessing the Achilles tendon reflexes [8].

The advancement in infrared camera technology has revolutionised the field of measuring temperature whereby it is now being widely used for medical purposes [9]. The IR thermography is fast, nonintrusive and non-contact method. It is also passive in which no harmful radiation passes through the body and captures only body heat radiation [9]. In this study, we are using IR thermography for the detection of complications related to diabetic foot based on the plantar temperature distribution. This plantar temperature distribution provides details related to blood perfusion impairment [10], which is typical among the diabetic patients [11]. During the conditions when the blood circulation is significantly reduced (ischemic), especially at the periphery limbs, the temperature pattern will change [12]. The IR thermography is contactless and hence has the advantage over the other assessment tools such as the monofilament and vibration sensation tests [13]. It limits the unnecessary contact and pressure that may affect the temperature reading and mitigate the spread of infection through the apparatus [14]. Moreover, it permits the measurement of temperature distribution of the whole foot regardless of the shapes or surfaces, particularly the medial arch which is a non-contact surface of the foot. Hence, analyzing the plantar temperature distribution can be effective for early detection of diabetic foot complications.

Infrared thermography has been used in many diabetic foot studies that relate plantar temperature variations with diabetic foot linked complications [15]. These studies are further categorised as separate lower limb temperature, asymmetric temperature, temperature distribution and, independent thermal and physical stress analysis. The separate lower limb temperature analysis in Table 1 represent the temperature ranges for the respective study groups. In 2010, Bagavathiappan et al. [16] studied the relationship between diabetic neuropathy patients and foot temperature. The study observed that diabetic neuropathy patient recorded highest foot temperature (32–35 °C) than non-neuropathy diabetes patients (27–30 °C). Also, diabetic neuropathy patients have higher mean foot temperature (MFT). Table 2 presents the studies on asymmetric analysis of diabetic foot thermograms. In general, the asymmetric temperature analysis compares the temperature between one foot and the contralateral foot. Liu et al. [17] performed an asymmetric analysis technique using coloured image segmentation and non-rigid landmark based registration B-splines of the right and left foot. The proposed method was able to detect diabetic foot ulcers and including all Charcot foot. Meanwhile, studies on temperature distribution analysis are summarised in Table 3. Both Nagase et al. [14] and Bharara et al. [18] proposed a characterization technique for plantar thermography patterns based on plantar angiosomes concept. The drawbacks may be the bias of variations in the control group due to smaller number of participants. The gender and age are unmatched in the control group, which may lead to confounding factors for data interpretation. Besides, the proposed manual classification method of 20 categories may not be suitable for clinical purposes. The studies based on independent thermal and physical stress analysis prior to thermogram acquisition is depicted in Table 4. In 2015, Agurto et al. [19] proposed a method to classify diabetic peripheral neuropathy patients using IR thermography and independent component analysis (ICA) method. The limitations are that few initial frames are not considered for the analysis and some areas, particularly the toes, present artefacts which require stabilizing the toes to avoid significant movements. Therefore, continuous development of algorithms is needed to better determine and analyse the thermal changes in the diabetic foot.

The purpose of this study is to develop an early detection system for diabetic foot using plantar foot thermograms. The plantar thermal patterns and distributions among the normal and diabetes subjects are analyzed and classified. The proposed system can be introduced as a screening tool in diabetic clinic to provide clinician with medical supports in diagnosing the magnitude of diabetic foot cases. In this proposed system, the normal and diabetic plantar foot thermograms are first segmented and warped. These warped foot images are subjected to discrete wavelet transform (DWT) and higher order spectra (HOS) techniques and then various texture and entropy features are extracted from the coefficients. The combined extracted features are ranked using t-values. Then these ranked features are fed to the SVM classifier for automated classification.

2. Materials & methodology

2.1. Population study

The normal and diabetes without neuropathy groups were considered in this study. A total of 33 healthy subjects and 33 non-neuropathic diabetic patients were recruited from Ngee Ann Polytechnic and Singapore General Hospital (SGH), Diabetes & Metabolism Centre (DMC) respectively under identical conditions. The diabetic foot thermograms data collection has been approved by SingHealth Centralised Institutional Review Board (CIRB) **(CIRB Ref: 2016/3044)** while normal foot thermograms data collection has been approved by Ngee Ann Polytechnic-Institutional Review Board (NP-IRB) **(NPIRB-P0175-2017-ECE-AMA6)**. The details of diabetes and normal groups are presented in Table 5. The participants in both groups were informed about the study prior to obtaining inform consent from them. Importantly, participants with past ulcerations or amputation, peripheral vascular disease, ischemic heart disease and neurological disorder were excluded.

2.2. Acquisition of thermogram

The plantar foot thermograms acquisition was carry out in a controlled room temperature of 20 ± 1 °C and humidity of

Table 1
Separate lower limb temperature analysis using IR thermography.

Reference (Year)	Methodology	Findings
Ammer et al. (2001) [20]	• Physical examination of feet • Neurological assessment • Thermal imaging • Single Measure Intraclass Correlation • Mann-Whitney *U* test	• No relationship between skin changes and increased skin temperature
Melnizky et al. (2002) [21]	• Physical examination of feet • Nerve conduction test • Thermal imaging • SPSS 10.0 for statistical analysis	• A pathological temperature gradient was detected on the right limb of 36 diabetes patients (mean pathological gradient: -0.27 ± 0.68 K vs -1.84 ± 0.81 K) whereas 39 patients on the left limb (-0.77 ± 1.15 Kvs -1.49 ± 1.21 K) • No correlation between temperature measurements and nerve conduction
Sun et al. (2005) [22]	• Electromyography for sympathetic skin response (SSR) test • Thermal imaging • Compute average temperature of six sub regions on each healthy sole • Analyze sole temperature normalization relative to forehead temperature of diabetes patients • SPSS for statistical analysis	• Highest temperature (29.3 ± 0.9 °C) in the arc areas and lowest for the toes (26.2 ± 1.2 °C). • Diabetes patients without sympathetic skin response (SSR) had higher mean plantar temperature (27.6 ± 1.8 °C) compared to those with SSR (26.8 ± 2.2 °C) • Equilibrium temperature is achieved at mean plantar temperature (27.8 ± 1.0 °C) after 15 min
Sun et al. (2006) [23]	• Seattle Wound Classification system • Thermal imaging • Electromyography for sympathetic skin response (SSR) test • Neurological assessment • SPSS for statistical analysis	• At risk diabetes patients with pre-ulcerative skin and without SSR had highest mean foot temperature (30.2 ± 1.3 °C) compared to diabetes patients without SSR (27.9 ± 1.7 °C), diabetes patients with SSR (27.1 ± 2.0 °C), and normal subjects (26.8 ± 1.8 °C)
Sun et al. (2008) [24]	• Seattle Wound Classification system • Thermal imaging • Electromyography for sympathetic skin response (SSR) test • Neurological assessment • Nerve conduction test • SPSS for statistical analysis	• At-risk class is 13.4 times more likely to develop plantar ulcerations than the diabetes patients with and without SSR during the 4-year period
Nishide et al. (2009) [25]	• Ankle Brachial Index (ABI) • Toe Brachial Index (TBI) • Achilles tendon reflex and vibratory perception • Semmes-Weinstein monofilament test • Thermography • Ultrasonography • Fisher's exact probability test • Mann-Whitney *U* test • SPSS for statistical analysis	• Ultrasonography and thermography detect inflammation symptoms in 10% of the calli in diabetes class whereas no inflammation detected in the normal class.
Bharara et al. (2010) [26]	• Thermal imaging • Thermal index • Image J Software	• Thermal index/wound inflammatory index moved from negative to positive ($p < .05$) prior to reaching zero
Bagavathiappan et al. (2010) [16]	• Anthropometric measurements • Glycated hemoglobin (HbA1c) • Neuropathy assessment • Vascular sufficiency assessment • Thermal imaging • SPSS for statistical analysis	• Diabetes neuropathy patients recorded highest foot temperature (32–35 °C) than non-neuropathy diabetes patients (27–30 °C) • Higher mean foot temperature (MFT) for Diabetes neuropathy patients • No relationship between MFT and glycated hemoglobin

55 ± 5%. The subjects were required to remove their foot wears, socks, and the feet were cleaned. The subjects then remained seated in a supine position on the treatment bench for about 15 min. The purpose is to reach thermal equilibrium prior to capturing the thermogram. The segmented thermograms of normal and diabetic feet seen in Fig. 1(a) and (b) were captured by the Thermographic System VarioCAM© hr head 680/30 mm. The infrared camera was placed at focus distance of 1 m from the feet. The acquired foot plantar thermogram was presented in RGB (Red, Green, and Blue) Color space with temperature scale ranging from 24 to 32 °C. The infrared camera automatically calibrates the temperature scale based on the coldest and hottest points in the scene. The thermograms are kept in ***irbis*** format after acquisition and thereafter converted into ***bmp*** format for subsequent image analysis.

2.3. Methodology

All the segmented foot thermograms undergo warping process that transform the segmented region into a standard shape and size [52]. The temperature data contained in the segmented region is decomposed using DWT and HOS methods. The DWT and HOS features are able to capture the minute sudden variations between the adjacent pixels and, the non-linear interaction in the phase coupling and frequency components respectively [53]. Subsequently, feature values extracted from bilateral foot are subtracted and then classified using SVM classifier. The block diagram of the proposed system is shown in Fig. 2.

2.3.1. Segmentation of plantar foot

The normal and diabetic plantar foot regions are first segmented. The plantar foot region is manually delineated using polygon with 16 chosen points. These points are positioned on the boundary of the foot. These points are then joined by straight lines that enclosed the entire plantar foot including the toes. The segmented left foot is flipped in the same orientation as right foot for equal comparison prior to subsequent analysis. The delineation and selection of plantar foot region of interest (ROI) is demonstrated in Fig. 3(a) and (b) respectively.

Table 2
Asymmetric temperature analysis using IR thermography.

Reference (Year)	Methodology	Findings
Harding et al. (1998) [27]	• Infrared imaging • Radiography	• Out of the 26 diabetes patients with positive thermograms, 21 of whom are confirmed with osteomyelitis by radiological evidence • Positive thermogram is described as at least 0.5 °C rise in temperature of the affected foot skin with respect to the contralateral foot sole
Kaabouch et al. (2009a) [28]	• Infrared imaging • Segmentation • Geometric transformation • Asymmetry analysis	• Able to detect and determine inflammation and ulcers accurately and rapidly
Kaabouch et al. (2009b) [29]	• Infrared imaging • Automatic thresholding • Geometric transformation • Asymmetry analysis • Features extraction	• Genetic algorithm yields superior thresholding results • Low and high order statistics effectively enhance the asymmetry analysis in detecting foot abnormalities
Kaabouch et al. (2010) [30]	• Infrared imaging • Segmentation • Geometric transformation • Asymmetry analysis	• Genetic algorithm produces superior thresholding results
Kaabouch et al. (2011a) [31]	• Infrared imaging • Segmentation • Geometric transformation • Asymmetry analysis and abnormality identification • Features extraction	• Genetic algorithm produces superior thresholding results • Low and high order statistics effectively enhance the asymmetry analysis in detecting foot abnormalities
Kaabouch et al. (2011b) [32]	• Infrared imaging • Genetic algorithms • Asymmetry analysis-based scalable scanning	• Genetic algorithms effectively crop the feet from background and eliminate most noise • Scalable scanning method yield fewer false abnormal regions
Liu et al. (2013) [33]	• Infrared imaging • Foot segmentation • Feet registration • Abnormal detection	• Active contours without edges method acquire reasonable result • Automated detection of pre-symptoms ulceration by computing temperature difference of the feet • 2.2 °C as the clinical relevant difference
Peregrina-Barreto et al. (2013) [34]	• Infrared imaging • Color characterization • Foot angiosomes and color classification	• The temperature estimate difference between corresponding angiosomes can be used to screen for abnormality
van Netten et al. (2013) [35]	• Infrared imaging • Mean temperature of whole foot and regions of interest	• Mean temperature of contralateral and ipsilateral foot is the same in patients with localized problems • Temperature at ROI was more than 2 °C compared to the similar area in contralateral foot and to the mean of the entire ipsilateral foot • Mean temperature differences between the contralateral and ipsilateral foot was more than 3 °C in patients with diffuse problems
Peregrina-Barreto et al. (2014) [36]	• Infrared imaging • Color characterization • Temperature estimated difference • Hot spots detection	• HSE capable of detecting abnormal small areas in the early phase that were not detected by ETD estimator
van Netten et al. (2014) [37]	• Infrared imaging • Clinical foot assessments • Kruskal-Wallis test • Receiver operating characteristic (ROC) curve and area using SPSS	• Optimal cut-off value for skin temperature in identifying diabetes foot problems was difference of 2.2 °C between contralateral spots, with 76% sensitivity and 40% specificity • Optimal cut-off values for skin temperature to decide the urgency for treatment was difference of 3.5 °C between left and right foot mean temperature, with 89% sensitivity and 78% specificity
Vilcahuaman et al. (2014) [38]	• Infrared imaging • Image processing	• In the clinical study, 10% of the diabetes patients had signs of significant hyperthermia on the foot plantar with temperature difference of more than 2.2 °C
Vilcahuaman et al. (2015) [39]	• Infrared imaging • Image processing	• High risk group had significantly higher temperature (32 ± 2 °C) than medium risk group (31 ± 2 °C) • In the study, 9 out of 82 diabetes patients had significant hyperthermia
Liu et al. (2015) [17]	• Infrared imaging • Foot segmentation • Registration optimization • Asymmetric analysis	• The study yielded an accuracy of 95% with 35 out of the 37 diabetic foot ulcers identified • All three Charcot feet are successfully detected

2.3.2. Higher order spectra (HOS)

The warped grayscale foot images are subjected to Radon transform [54,55] which coverts these images into one dimensional data prior to HOS. HOS comprised of higher order cumulants and moments spectra of a signal [56]. In this study, features are extracted from third order statistics known as bispectrum by Fourier transforming the third order correlation. The features in this study is based on the phases of integrated bispectrum [57] which yield HOS coefficients. The bispectral invariant features are being used for every 5°. Typical bispectrum and bispectrum contour plots of diabetic and normal foot are shown in Figs. 4(a)–(d) and 5(a)–(d) respectively.

2.3.3. Discrete wavelet transform (DWT)

Discrete wavelet transform (DWT) transforms a two-dimensional signal by subjecting through a series of down sam-

Table 3
Temperature distribution analysis.

Reference (Year)	Methodology	Findings
Branemark et al. (1967) [40]	• Infrared imaging • Clinical assessment	• Abnormal emission patterns from hand and feet of all diabetes patients • Reduced emission on the metatarsal and toes areas
Nagase et al. (2011) [14]	• Infrared imaging • Conceptual classification comprising of 20 categories of plantar thermography patterns	**Normal** • 48 feet (or 75%) are characterized to the seven categories and the remaining 16 feet characterized as atypical • The Id category (butterfly pattern) is mostly identified with 30 feet (or 46.9%)**Diabetes** • 225 (or 87.2%) diabetes feet are characterized to 18 categories and the remaining 33 feet (or 12.8%) as atypical • The IIa category (medial and lateral plantar arteries undamaged) is mostly identified with 101 feet (or 39.1%)
Oe et al. (2013) [41]	• MRI scans • Infrared imaging • Ankle-brachial index (ABI) • Toe-brachial index (TBI) • Nerve conduction velocity • SPSS for statistical analysis	• Ankle pattern is mostly common in patients with osteomyelitis • Sensitivity = 60% • Specificity = 100% • PPV = 100% • NPV = 71.4%
Mori et al. (2013) [42]	• Ankle-brachial index (ABI) • Toe-brachial index (TBI) • Achilles tendon reflex • Semmes-Weinstein monofilament test • Vibratory sensation test • Infrared imaging • Image partitioning algorithm • T test or chi square test	**Normal** • 47 feet are characterized to the four categories and the remaining 17 feet characterized as anomalous • The type 1 (butterfly pattern) (44%) is mostly identified **Diabetes** • 198 diabetes feet are characterized to six categories and the remaining 60 feet as atypical • The type 2 (46%) is mostly identified
Bharara et al. (2014) [18]	• Clinical assessment • Semmes Weinstein monofilament • Vibratory perception threshold • Infrared imaging	**Normal** • Subjects are mostly represented by Id category (Butterfly Pattern) during measurements with 47.2% at rest, 13.8% at post stress and 27.8% at recovery **Diabetes** • Subjects are mostly represented by IIa category (medial and lateral plantar arteries undamaged) during measurements with 50% at rest, 50% at post stress and 28.57% at recovery
Hernandez-Contreras et al. (2015a) [43]	• Infrared imaging • Grayscale characterization • Arch segmentation based on histogram distribution • Mathematical morphology	**Normal** • Butterfly pattern is presented in the subjects and pattern spectrum is same as oval • Mean percentage of pixels for control group is highest in quadrant 4 with 88.05% **Diabetes** • Pattern spectrum is irregular due to the dissimilar pattern • Mean percentage of pixels is 28.87% for diabetes group in quadrant 3
Hernandez-Contreras et al. (2015b) [11]	• Infrared imaging • Grayscale characterization • Foot segmentation • Temperature pattern • Mathematical morphology • Pattern spectrum • Multilayer perceptron • K-fold cross validation	• Proposed technique achieved average classification rate of 94.33%

pling of low and high pass filters [58]. The rows are put through the high and low pass filters to yield the high (H) and low (L) frequency components respectively. A two-level DWT decomposition of an image is illustrated in Fig. 6. In this study, the normal and diabetic foot images undergo two level of DWT decomposition using Daubechies 8 (db8) mother wavelet [59] as shown in Fig. 7(a) and (b).

2.3.4. Feature extraction

For this study, texture and entropy based features are extracted from the decomposed DWT and HOS images. The feature extraction techniques employed are gray level co-occurrence matrix (GLCM) [60], Hu's invariant moment [61], local binary pattern (LBP) [62], Laws texture energy (LTE) [63] and entropies [64–70]. The feature values extracted from both left and right foot are subtracted and the resultant feature value obtained are then ranked using p-value, analyzed and classified.

2.3.5. Student t test

The student t test is used to identify distinctive features by analyzing the p-value. The p-value provides an indication if the *means* of the two groups are statistically distinct [71]. A low p-value provides the confidence that the feature is more clinically distinct [72]. In this study, the performance of the feature for the proposed system is evaluated by ranking the p-value in ascending order and subsequently applying the ranked features independently into the classifier until maximum accuracy is obtained.

2.3.6. Support vector Machine (SVM)

It is a two-class classifier that uses support vectors to solve various types of classification problems [73,74]. This technique determines the hyperplane which acts as a decision surface. The hyperplane divides the data points belonging to the classes with maximum margin. In this study, nonlinear kernel functions namely polynomial and radial basis functions (RBF) combined with SVM classifier are able to better separate the nonlinear features and hence yielding maximum classification performance. The set of points are mapped into a higher dimension space that allows the separation of the points with nonlinear kernel functions [73]. Then ten-fold cross validation is used to train and test the SVM classifier [75].

3. Results

The student t test is used to select the significant features for accurate discrimination between normal and diabetic groups. From the total combination of 4810 features, only 27 clinically signifi-

Table 4
Independent thermal and physical stress analysis.

Reference (Year)	Methodology	Findings
Fushimi et al. (1996) [44]	• ECG • Ankle pressure index • Infrared imaging • Ultrasonic imaging	**Normal** • All subjects had normal pattern **Diabetes** • 43 had normal, 19 increasing and 26 decreasing and 24 flat patterns
Fujiwara et al. (2000) [45]	• Infrared imaging • Ankle-brachial index • Doppler meter • Motor nerve conduction velocity • Sensory nerve conduction velocity • ECG • Schellong's test • Photo-dispersion method • ANOVA with Neuman-Keuls multiple comparison test	• Smaller skin temperature drops in diabetes patients compared to normal subjects after immersing into cold water • Diabetes patients had lower skin temperature recovery rate due to causal factors such as peripheral arterial sclerosis, abnormal blood coagulation fibrinolysis and sympathetic nerve dysfunction
Hosaki et al. (2002) [46]	• Infrared imaging • Laser Doppler blood flowmeter • Hot loading at 36 °C • Cold loading at 20 °C • Compute recovery ratio	• Recovery ratios for the 27 diabetes patients were in the range of 0–93.5% and the average was 34% • Blood flow and recovery ratio were correlated (r = 0.634, p < .0001) • Ratio of blood flow after cold loading over the blood flow after hot loading was in the range of 38.1–122% and average of 80.6%. • This ratio and recovery ratio is correlated (r = 0.502, p < .0001)
Balbinot et al. (2012) [47]	• Clinical assessments • Heart rate variability • Infrared imaging • Electromyography • Statistical analysis	**Diabetes** • Interdigital anisothermal method performed better than thermal recovery index with 46.2% specificity and 81.3% sensitivity **Prediabetes** • All three tests achieved 25% specificity and 80% sensitivity equally
Barriga et al. (2012) [48]	• Infrared imaging • Motion tracking of thermal features • Exponential curve fitting	• Diabetes neuropathy patient recorded recovery rate of 2% at the two toes and approximately 0.4% at the heel • Normal subject recorded high recovery of 4% at the medial arch as compared to <1.5% in the diabetes neuropathy patient
Najafi et al. (2012) [49]	• Two pre-defined paths of 50 and 150 steps • Infrared imaging • Image processing • Student *t* test • ANOVA	• In Charcot neuroarthropathy group, the decreased in temperature for non-affected foot is 1.9 folds more than the affected foot • Plantar temperature for both foot in Charcot neuroarthropathy group significantly increased beyond 50 steps and remain higher on the affected foot at 200 steps
Balbinot et al. (2013) [50]	• Clinical assessments • Infrared imaging • Data analysis • Statistical analysis	• Significant difference in the average temperatures of normal subjects between the two days before and after cold stress test compared to no difference in the average temperatures for diabetes patients • Rewarming index of both groups did not differ between the two days
Yavuz et al. (2014) [51]	• Walking on pressure shear plate • Treadmill walking • Infrared imaging • Peak shear stress and peak resultant stress • Statistical analysis	• Significant correlation between temperature rises and peak shear stress (r = 0.78) • Increased in plantar temperature can predict the site of peak resultant stress and peak shear stress in 39% and 23% of the subjects
Agurto et al. (2015) [19]	• Cold stimulus • Infrared imaging • Independent component analysis (ICA)	• Components 2, 6 and 8 significantly differentiate the normal and diabetes peripheral neuropathy patients • Higher recovery rate in normal subjects for component 6 • Diabetes peripheral neuropathy patients have lower temperature recovery rate in most parts of the foot plantar

Table 5
Demographic information of normal and diabetes groups (mean ± standard deviation).

	Normal group	Diabetes group
Subjects	33	33
Female	15	15
Male	18	18
Average age (years)	51.94 ± 11.25	56.18 ± 14.71
Average Body Mass Index (BMI) (kg/m^2)	23.50 ± 3.61	25.08 ± 5.31

cant features (with *p* value < .0001) are chosen. In Table 6, the *mean*, standard deviation and *p* value of these significant features are tabulated. The cH2_LME22 and 2_HOS36 have the lowest (.00002) and highest (.00014) *p* values respectively. These significant features registered higher *mean* value for normal group as compared to diabetes group. This clearly indicates a discrimination between the *two* groups. The cH2_LME22 feature is acquired from the 22nd coefficient of law mask energy extracted from the second level horizontal coefficient of DWT. In contrast, the 2_HOS36 feature is obtained from the 36th coefficient of HOS at 5° (2nd angle). The bar plot of 27 significant features (p < .0001) for normal and diabetes foot thermal images are shown in Fig. 8(a) and (b).

The ranked significant features are individually fed into SVM classifier. In Table 7, the first column denotes the number of features fed into the classifier. The subsequent *four* columns indicate the number of True Positive (TP), True Negative (TN), False Positive (FP) and False Negative (FN). The classification accuracy, positive predictive value (PPV), sensitivity and specificity are shown in columns 6, 7, 8, and 9 respectively. The SVM classifier with RBF kernel function yielded highest classification accuracy of 89.39%, PPV of 96.43%, sensitivity of 81.81% and specificity of 96.97% using five features. As the features become less significance down the ranked, the classification performance also drops. The plot of accuracy (%)

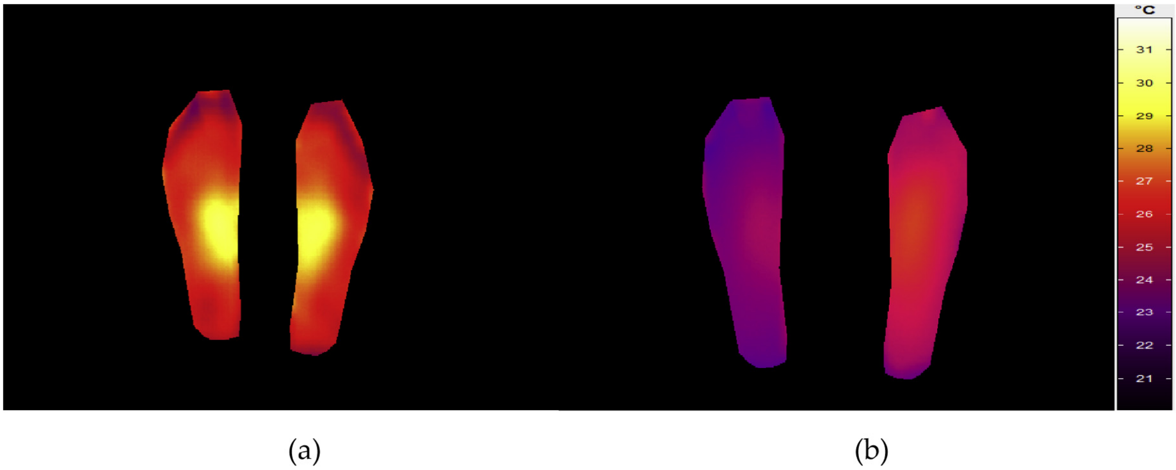

Fig. 1. (a) - (b) The segmented feet thermograms (°C) of (a) normal and (b) diabetes without neuropathy.

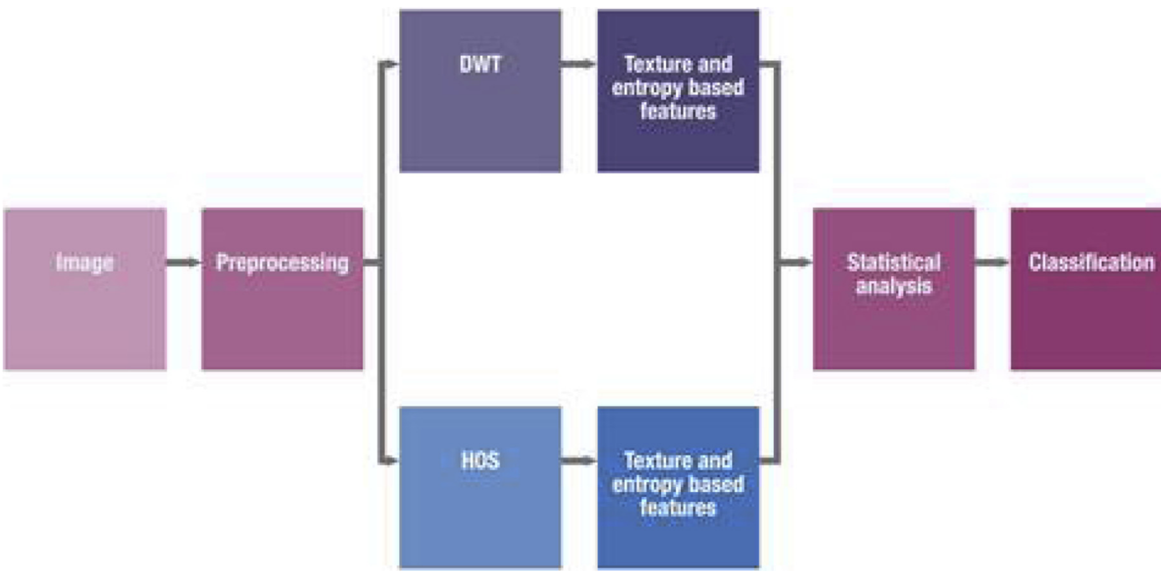

Fig. 2. Block diagram of the proposed methodology for automated diabetic foot detection.

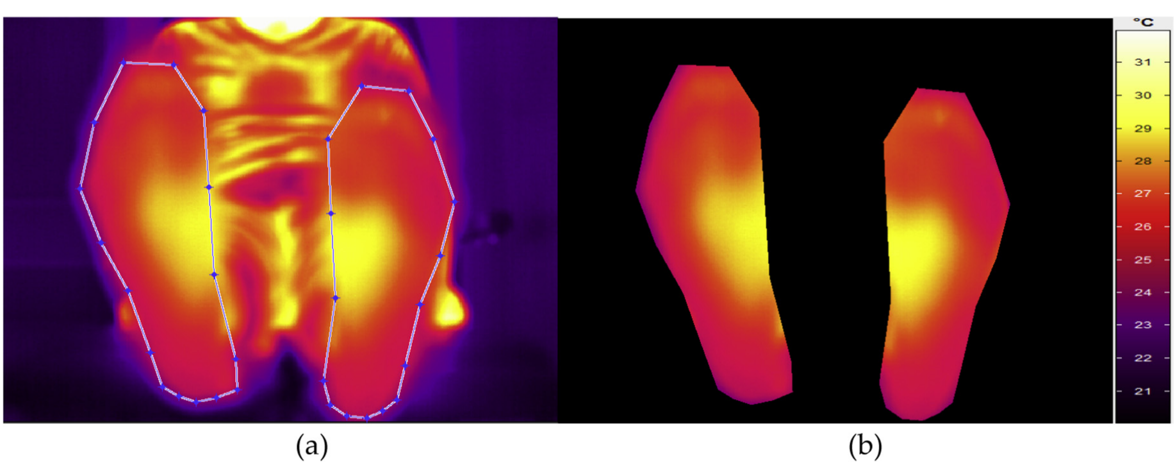

Fig. 3. (a)-(b) Segmentation of plantar foot segmentation: (a) delineation using polygon. (b) region of interest.

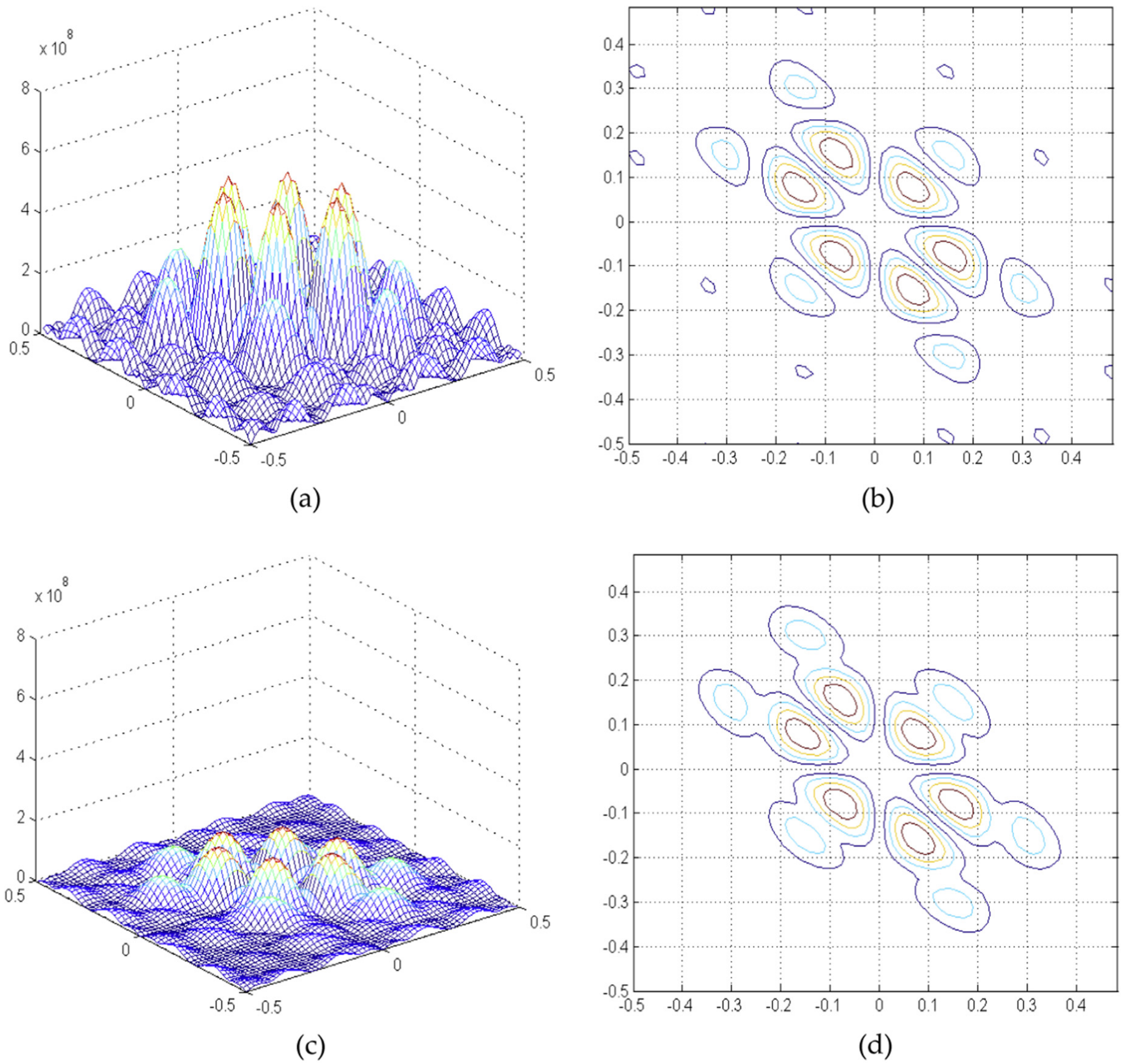

Fig. 4. (a)-(d) Typical plot of diabetic foot. Left foot: (a) bispectrum, (b) bispectrum contour. Right foot: (c) bispectrum, (d) bispectrum contour.

against the number of features using SVM classifier is presented in Fig. 9. Also, the classification performance across the ten folds is shown in Fig. 10.

4. Discussion

The IR thermography coupled with advances in image processing techniques have paved the way for obtaining unique thermal patterns for various classes and automated characterization of plantar foot thermograms [76]. The various studies conducted using IR thermography for the analysis of diabetic foot are presented in Tables 1–4. The majority of these studies are conducted using clinical parameters. It may not be easy to capture the subtle abnormal temperature variations through visual examination of the thermograms [77]. Hence, we have developed an automated detection system to help the clinicians.

In our study, DWT and HOS coefficients can capture the minute sudden changes in the pixels efficiently [53]. Evidently (Table 6), diabetes group has lower features compared to normal group. This indicates that the changes in the pixel values of diabetic IR thermograms are subtle and contains less high frequency components. This can be seen from the bispectrum plot of diabetic and normal foot in Figs. 4(a)–(d) and 5(a)–(d) respectively. The diabetic foot show lower bispectrum amplitude (z-axis) and thus lower feature values after subtraction of left and right foot features values. From Table 6, the cH2_LME22 features obtained from the second level horizontal coefficient of DWT are ranked high with diabetic foot having low feature values. It can be seen in Fig. 7(a) and (b) that there are not much sudden changes in the second level horizontal coefficient for diabetes as compared to normal. Hence, these feature values are relatively low for diabetes compared to normal foot.

The significant features in Table 6 are mostly HOS based features. The HOS method is able to better captures information relating to the nonlinearity and phase present in the diabetic foot images. These features are thus highly distinctive and discriminative as compared to DWT. Furthermore, they are significantly robust in noisy environment and hence, effective in capturing the non-linear interaction of the pixels in the phase coupling and frequency domain [53]. Also, it is able to capture the sudden changes in the image efficiently [78].

In the diabetes group, the decrease in blood circulation to the foot may be due to developing peripheral arterial disease which result in cold plantar foot thermogram [79]. This is represented with less intensity and subtle variability in the pixels of entire

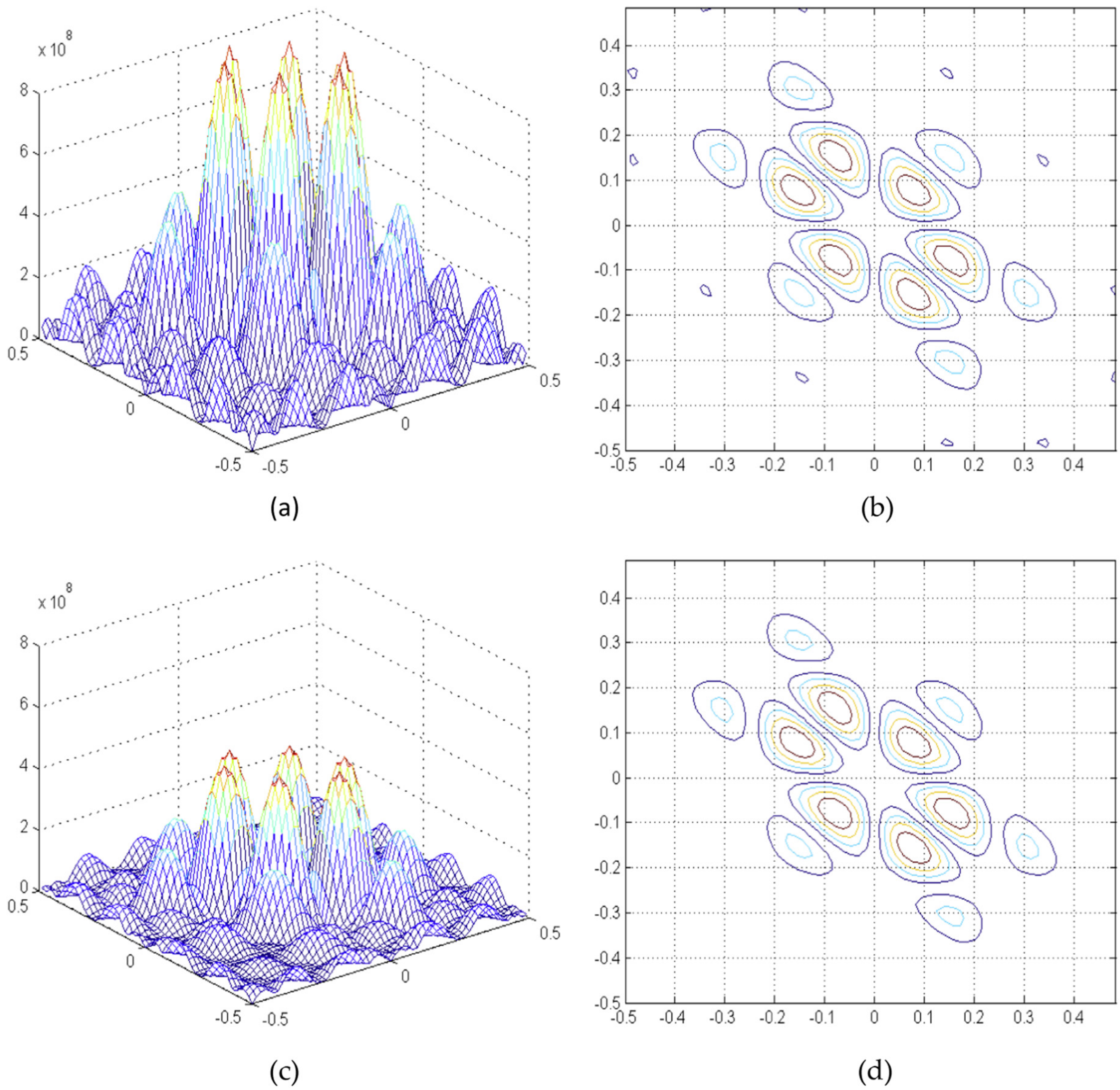

Fig. 5. (a)-(d) Typical plot of normal foot. Left foot: (a) bispectrum, (b) bispectrum contour. Right foot: (c) bispectrum, (d) bispectrum contour.

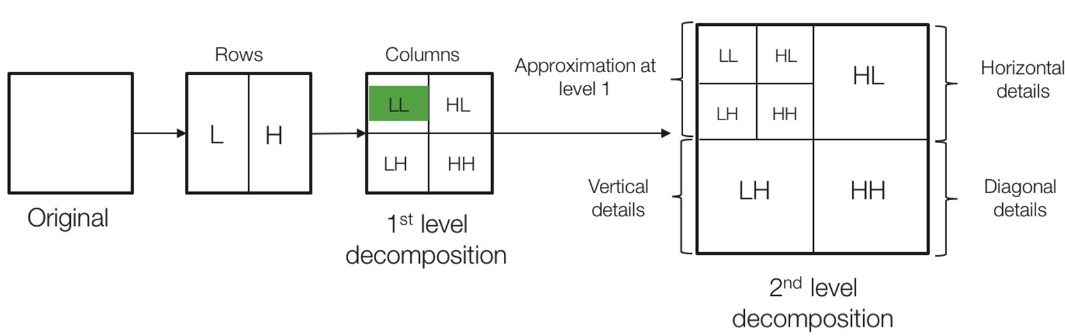

Fig. 6. An illustration of two-dimensional DWT of two level.

diabetic foot thermogram. In this study, textures and entropies are used to effectively capture variations in the pixels from the HOS and DWT coefficients.

The advantages of the proposed methodology are given below:

1. Method is simple, easy, and accurate.
2. Acquired maximum accuracy of 89.39%, sensitivity of 81.81%, and specificity of 96.97%. Thus, our method is fast as it used only five features to achieve the highest performance.
3. Proposed method is reliable as we have taken the same number of subjects with matching age groups and gender.
4. Obtained clear thermal patterns for the two classes (Fig. 1).

Table 6
Features extracted for normal and diabetes groups (***p*** < **.0001**).

Feature	Normal		Diabetes		*t*-Value
	Mean	Standard Deviation	Mean	Standard Deviation	
cH2_LME22	0.4000	0.2785	0.1611	0.1094	4.5851
34_HOS119	0.4314	0.2028	0.2186	0.1819	4.4861
3_HOS107	0.4034	0.3023	0.1557	0.1274	4.3378
19_HOS56	0.2428	0.2234	0.0665	0.0718	4.3166
2_HOS94	0.3166	0.2674	0.1096	0.0813	4.2548
36_HOS44	0.4069	0.3055	0.1584	0.1413	4.2413
36_HOS52	0.4116	0.3068	0.1624	0.1425	4.2324
19_HOS67	0.2219	0.2101	0.0619	0.0603	4.2064
36_HOS61	0.4013	0.3015	0.1581	0.1404	4.2007
2_HOS93	0.3094	0.2634	0.1075	0.0851	4.1887
2_HOS44	0.2966	0.2620	0.0998	0.0709	4.1647
cH2_LME21	0.3342	0.2692	0.1250	0.1044	4.1613
2d_HOS52	0.2984	0.2642	0.1007	0.0718	4.1466
20_HOS4	0.3181	0.2869	0.0916	0.1275	4.1450
2_HOS81	0.2947	0.2612	0.0979	0.0821	4.1298
36_HOS71	0.3816	0.2891	0.1530	0.1344	4.1182
2_HOS61	0.3037	0.2693	0.1045	0.0737	4.0987
2_HOS70	0.2878	0.2592	0.0943	0.0807	4.0949
36_HOS82	0.3546	0.2697	0.1427	0.1266	4.0861
19_HOS37	0.2055	0.1946	0.0611	0.0582	4.0832
2_HOS71	0.3134	0.2788	0.1082	0.0775	4.0738
2_HOS60	0.2845	0.2576	0.0932	0.0799	4.0728
19_HOS46	0.2033	0.2029	0.0549	0.0525	4.0703
2_HOS51	0.2825	0.2567	0.0926	0.0794	4.0590
2_HOS43	0.2814	0.2562	0.0923	0.0792	4.0514
2_HOS82	0.3363	0.3000	0.1163	0.0857	4.0511
2_HOS36	0.2811	0.2560	0.0922	0.0791	4.0489

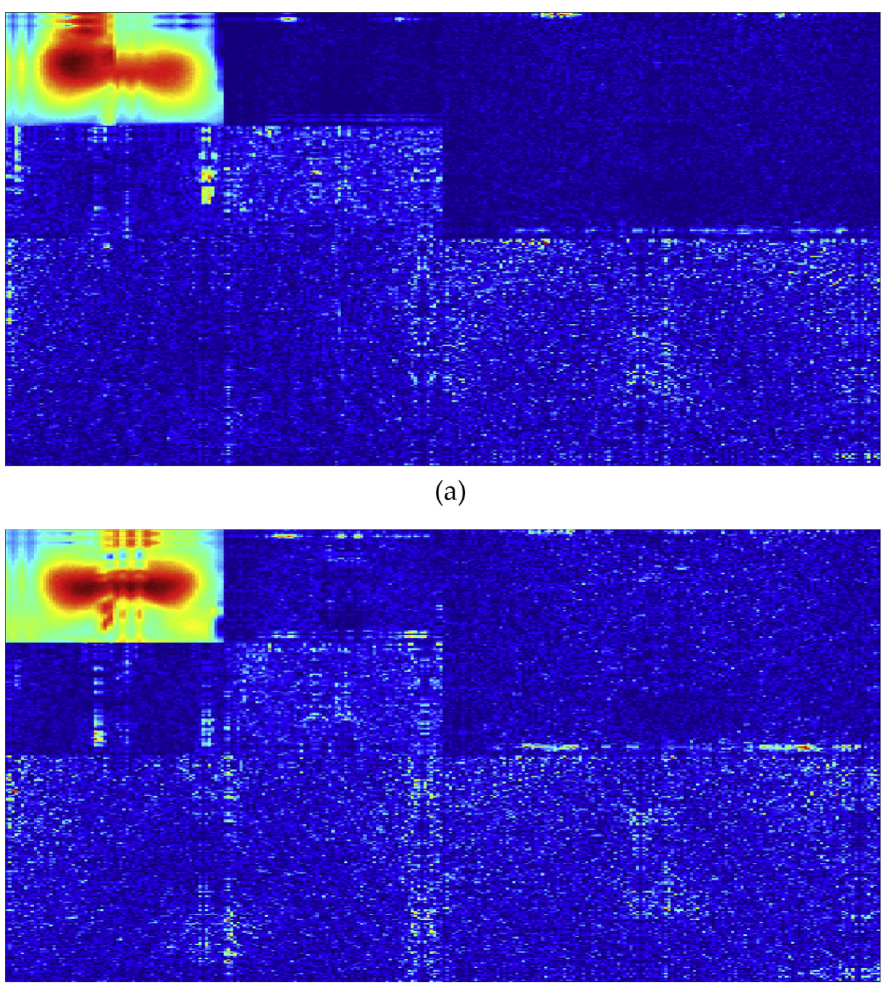

(a)

(b)

Fig. 7. (a)-(b) Two-level DWT of (a) diabetic and (b) normal foot thermogram.

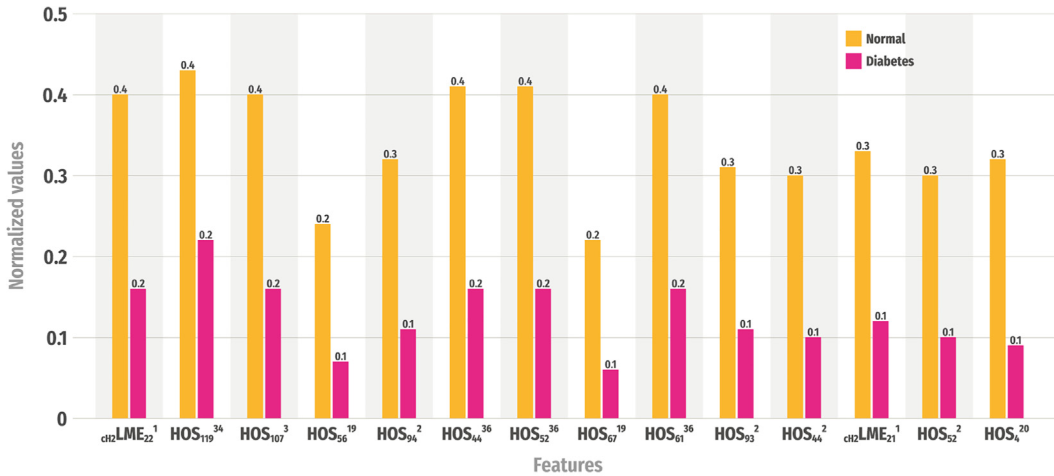

(a)

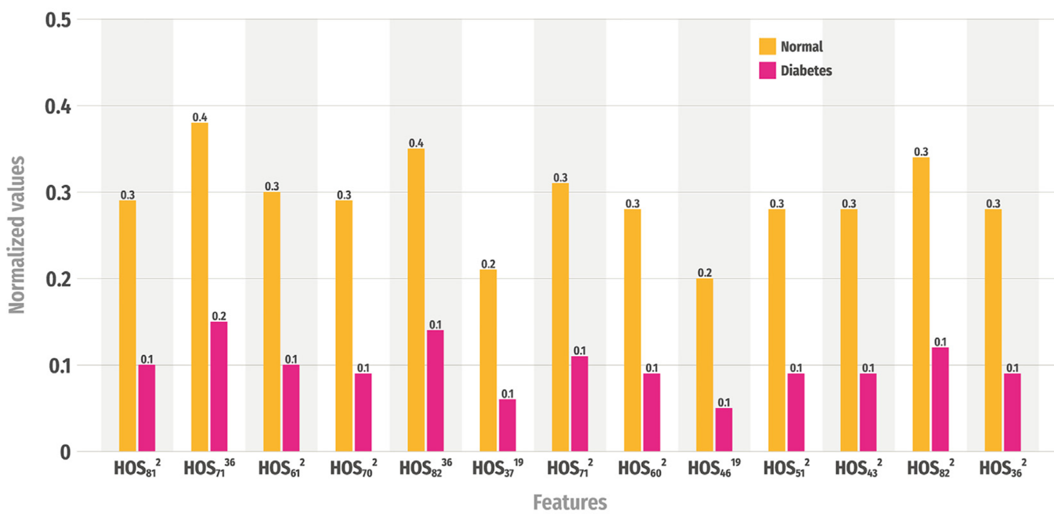

(b)

Fig. 8. (a)-(b) The results of 27 significant features ($p < .0001$) for normal and diabetes foot thermogram.

Table 7
Classification results with SVM classifier.

No. of features	TP	TN	FP	FN	Accuracy (%)	PPV (%)	Sensitivity (%)	Specificity (%)
2	29	27	6	4	84.85	82.86	87.88	81.82
3	29	27	6	4	84.85	82.86	87.88	81.82
4	25	33	0	8	87.88	100.00	75.76	100.00
5	27	32	1	6	89.39	96.43	81.82	96.97
6	26	33	0	7	89.39	100.00	78.79	100.00
7	24	33	0	9	86.36	100.00	72.73	100.00
8	25	33	0	8	87.88	100.00	75.76	100.00
9	24	33	0	9	86.36	100.00	72.73	100.00
10	26	31	2	7	86.36	92.86	78.79	93.94
11	25	31	2	8	84.85	92.59	75.76	93.94
12	26	32	1	7	87.88	96.30	78.79	96.97
13	26	32	1	7	87.88	96.30	78.79	96.97
14	25	32	1	8	86.36	96.15	75.76	96.97
15	25	31	2	8	84.85	92.59	75.76	93.94
16	24	32	1	9	84.85	96.00	72.73	96.97
17	25	31	2	8	84.85	92.59	75.76	93.94
18	26	30	3	7	84.85	89.66	78.79	90.91
19	23	32	1	10	83.33	95.83	69.70	96.97
20	24	32	1	9	84.85	96.00	72.73	96.97

TP = True Positive; **TN** = True Negative; **FP** = False Positive; **FN** = False Negative; **PPV** = Positive Predictive Value.

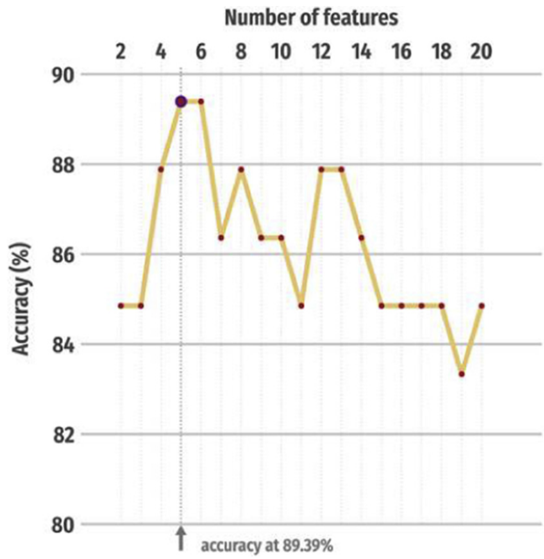

Fig. 9. Plot of accuracies (%) versus number of features with SVM classifier.

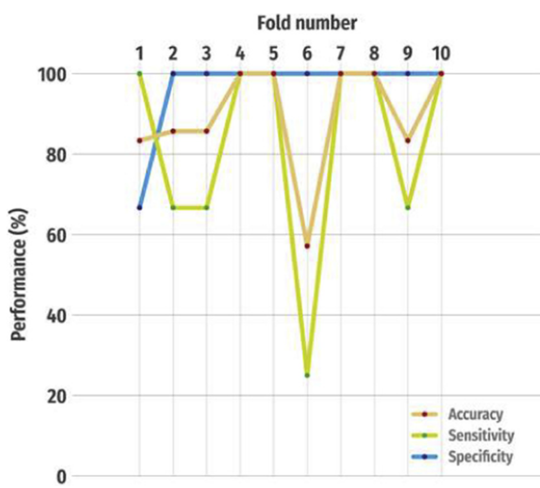

Fig. 10. Plot of performance (%) versus the number of folds.

The limitations of our proposed method include:

1. Used only 66 subjects (33 normal and 33 diabetes).
2. Semi-automated system.
3. IR thermography is expensive.

In future, we propose to use more subjects in each group and also make the system completely automated by using deep learning algorithm [80,81]. The work can be extended by taking the images using small portable less expensive IR camera.

5. Conclusion

The DM is a metabolic disorder causing problems in different parts of the human body. Diabetic foot is one of the expensive complications, causing disability and impairing the quality of life. Our proposed CAD system achieved a maximum classification accuracy of 89.39%, sensitivity of 81.81%, and specificity of 96.97% using only *five* features. The proposed system can be introduced in polyclinics as an adjunct instrument to help the podiatrists to validate their diagnosis with plantar foot. In future, we intend to improve the classification performance using more patients. Also, plan to use this algorithm in detecting the early stage of DM and diabetes with neuropathy.

References

[1] W.H. Organization, Definition, diagnosis and classification of diabetes mellitus and its complications: report of a WHO consultation. Part 1, Diagnosis and classification of diabetes mellitus, 1999.
[2] U.R. Acharya et al., Automated diagnosis of diabetes using entropies and diabetic index, J. Mech. Med. Biol. 16 (01) (2016) 1640008.
[3] C.D. Mathers, D. Loncar, Projections of global mortality and burden of disease from 2002 to 2030, PLoS Med. 3 (11) (2006) e442.
[4] J. Apelqvist, J. Larsson, What is the most effective way to reduce incidence of amputation in the diabetic foot?, Diabetes/Metabolism Res Rev. (2000) 16(S1).
[5] A.J. Boulton et al., The global burden of diabetic foot disease, The Lancet 366 (9498) (2005) 1719–1724.
[6] P. Leung, Diabetic foot ulcers—a comprehensive review, The Surgeon 5 (4) (2007) 219–231.
[7] R.E. Pecoraro, G.E. Reiber, E.M. Burgess, Pathways to diabetic limb amputation: basis for prevention, Diabetes Care 13 (5) (1990) 513–521.
[8] N. Schaper et al., Prevention and management of foot problems in diabetes: a Summary Guidance for Daily Practice 2015, based on the IWGDF Guidance Documents, Diabetes/Metabolism Res. Rev. 32 (S1) (2016) 7–15.
[9] B. Lahiri et al., Medical applications of infrared thermography: a review, Infrared Phys. Technol. 55 (4) (2012) 221–235.
[10] M. Etehadtavakol, E.Y.K. Ng, N. Kaabouch, Automatic segmentation of thermal images of diabetic-at-risk feet using the snakes algorithm, Infrared Phys. Technol. 86 (2017) 66–76.
[11] D. Hernandez-Contreras et al., Automatic classification of thermal patterns in diabetic foot based on morphological pattern spectrum, Infrared Phys. Technol. 73 (2015) 149–157.
[12] F. Ring, Thermal Imaging Today and its Relevance to diabetes, SAGE Publications, 2010.
[13] M. Adam, E.Y. Ng, J.H. Tan, M.L. Heng, J.W. Tong, U.R. Acharya, Computer aided diagnosis of diabetic foot using infrared thermography: a review, Computers in biology and medicine 91 (2017) 326–336.
[14] T. Nagase et al., Variations of plantar thermographic patterns in normal controls and non-ulcer diabetic patients: novel classification using angiosome concept, J. Plastic, Reconstruct. Aesthetic Surg. 64 (7) (2011) 860–866.
[15] D. Hernandez-Contreras et al., Narrative review: diabetic foot and infrared thermography, Infrared Phys. Technol. 78 (2016) 105–117.
[16] S. Bagavathiappan et al., Correlation between plantar foot temperature and diabetic neuropathy: a case study by using an infrared thermal imaging technique, J. Diabetes Sci. Technol. 4 (6) (2010) 1386–1392.
[17] C. Liu et al., Automatic detection of diabetic foot complications with infrared thermography by asymmetric analysis, J. Biomed. Opt. 20 (2) (2015), 026003-026003.
[18] M. Bharara et al., Applications of angiosome classification model for monitoring disease progression in the diabetic feet, Proceedings of the 2014 Summer Simulation Multiconference, Society for Computer Simulation International, 2014.
[19] C. Agurto et al., Characterization of diabetic peripheral neuropathy in infrared video sequences using independent component analysis, in: 2015 IEEE 25th International Workshop on Machine Learning for Signal Processing (MLSP). IEEE; 2015.
[20] K. Ammer et al., Thermal imaging of skin changes on the feet of type II diabetics, in: 2001 Conference Proceedings of the 23rd Annual International Conference of the IEEE Engineering in Medicine and Biology Society, 2001.
[21] P. Melnizky, K. Ammer, O. Rathkolb, Thermographic findings of the lower extremity in patients with Type II diabetes, Thermol. Int. 12 (2002) 107–114.
[22] P.-C. Sun, S.-H.E. Jao, C.-K. Cheng, Assessing foot temperature using infrared thermography, Foot & Ankle Int. 26 (10) (2005) 847–853.
[23] P.C. Sun et al., Relationship of skin temperature to sympathetic dysfunction in diabetic at-risk feet, Diabetes Res. Clin. Pract. 73 (1) (2006) 41–46.
[24] P.C. Sun et al., Thermoregulatory sudomotor dysfunction and diabetic neuropathy develop in parallel in at-risk feet, Diabet. Med. 25 (4) (2008) 413–418.
[25] K. Nishide et al., Ultrasonographic and thermographic screening for latent inflammation in diabetic foot callus, Diabet. Res. Clin. Pract. 85 (3) (2009) 304–309.
[26] M. Bharara et al., Wound inflammatory index: a "Proof of Concept" study to assess wound healing trajectory, J. Diabet. Sci. Technol. 4 (4) (2010) 773–779.
[27] J. Harding et al., Infrared imaging in diabetic foot ulceration, in: Engineering in Medicine and Biology Society, 1998. Proceedings of the 20th Annual International Conference of the IEEE. IEEE, 1998.
[28] N. Kaabouch et al., Asymmetry analysis based on genetic algorithms for the prediction of foot ulcers, in: VDA; 2009.
[29] N. Kaabouch, Early, et al., detection of foot ulcers through asymmetry analysis, Proc. SPIE (2009).
[30] N. Kaabouch et al., Predicting neuropathic ulceration: analysis of static temperature distributions in thermal images, J. Biomed. Opt. 15 (6) (2010), 061715–061715-6.

[31] N. Kaabouch et al., Enhancement of the asymmetry-based overlapping analysis through features extraction, J. Electron. Imaging 20 (1) (2011), 013012–013012-7.

[32] N. Kaabouch, W.C. Hu, Y. Chen, Alternative technique to asymmetry analysis-based overlapping for foot ulcer examination: Scalable scanning. arXiv preprint arXiv:1606.03578, 2016.

[33] C. Liu et al., Infrared dermal thermography on diabetic feet soles to predict ulcerations: a case study, 2013.

[34] H. Peregrina-Barreto et al., Thermal image processing for quantitative determination of temperature variations in plantar angiosomes. In: Instrumentation and Measurement Technology Conference (I2MTC), 2013 IEEE International. IEEE, 2013.

[35] J.J. van Netten et al., Infrared Thermal Imaging for Automated Detection of Diabetic Foot Complications, SAGE Publications Sage CA, Los Angeles, CA, 2013.

[36] H. Peregrina-Barreto, L.A. Morales-Hernandez, J.J. Rangel-Magdaleno, J.G. Avina-Cervantes, J.M. Ramirez-Cortes, R. Morales-Caporal, Quantitative estimation of temperature variations in plantar angiosomes: a study case for diabetic foot, Computational and mathematical methods in medicine 2014 (2014).

[37] J.J. van Netten et al., Diagnostic values for skin temperature assessment to detect diabetes-related foot complications, Diabet. Technol. Therapeut. 16 (11) (2014) 714–721.

[38] L. Vilcahuaman et al., Detection of diabetic foot hyperthermia by infrared imaging, in: Engineering in Medicine and Biology Society (EMBC), 2014 36th Annual International Conference of the IEEE. IEEE; 2014.

[39] L. Vilcahuaman et al., Automatic Analysis of Plantar Foot Thermal Images in at-Risk Type II Diabetes by Using an Infrared Camera. in World Congress on Medical Physics and Biomedical Engineering, June 7–12, 2015, Toronto, Canada. Springer, 2015.

[40] P.-I. Brånemark et al., Infrared thermography in diabetes mellitus a preliminary study, Diabetologia 3 (6) (1967) 529–532.

[41] M. Oe et al., Screening for osteomyelitis using thermography in patients with diabetic foot, Ulcers 2013 (2013).

[42] T. Mori et al., Morphological Pattern Classification System for Plantar Thermography of Patients with Diabetes, SAGE Publications Sage CA, Los Angeles, CA, 2013.

[43] D. Hernandez-Contreras et al., Evaluation of thermal patterns and distribution applied to the study of diabetic foot, in: 2015 IEEE International Instrumentation and Measurement Technology Conference (I2MTC) Proceedings, 2015.

[44] H. Fushimi et al., Abnormal vasoreaction of peripheral arteries to cold stimulus of both hands in diabetics, Diabet. Res. Clin. Pract. 32 (1–2) (1996) 55–59.

[45] Y. Fujiwara et al., Thermographic measurement of skin temperature recovery time of extremities in patients with type 2 diabetes mellitus, Exp. Clin. Endocrinol. Diabet. 108 (07) (2000) 463–469.

[46] Hosaki, Y., et al., Non-invasive study for peripheral circulation in patients with diabetes mellitus. 岡大三朝分院研究報告, 2002. 72: p. 31-37.

[47] L.F. Balbinot et al., Plantar thermography is useful in the early diagnosis of diabetic neuropathy, Clinics 67 (12) (2012) 1419–1425.

[48] E.S. Barriga et al., Computational basis for risk stratification of peripheral neuropathy from thermal imaging, in: Engineering in Medicine and Biology Society (EMBC), 2012 Annual International Conference of the IEEE. IEEE, 2012.

[49] B. Najafi, J.S. Wrobel, G. Grewal, R.A. Menzies, T.K. Talal, M. Zirie, D.G. Armstrong, Plantar temperature response to walking in diabetes with and without acute Charcot: the Charcot Activity Response Test, Journal of aging research 2012 (2012).

[50] L.F. Balbinot et al., Repeatability of Infrared Plantar Thermography in Diabetes Patients: a Pilot Study, SAGE Publications Sage CA, Los Angeles, CA, 2013.

[51] M. Yavuz et al., Temperature as a predictive tool for plantar triaxial loading, J. Biomech. 47 (15) (2014) 3767–3770.

[52] J.H. Tan, E.Y.K. Ng, U.R. Acharya, Evaluation of tear evaporation from ocular surface by functional infrared thermography, Med. Phys. 37 (11) (2010) 6022–6034.

[53] K.S. Vidya et al., Computer-aided diagnosis of myocardial infarction using ultrasound images with DWT, GLCM and HOS methods: a comparative study, Comput. Biol. Med. 62 (2015) 86–93.

[54] W. Gonzalez, R.E. Woods, Eddins, Digital Image Processing Using MATLAB, Prentice Hall, Third New Jersey, 2004.

[55] R. Acharya et al., Application of higher order spectra for the identification of diabetes retinopathy stages, J. Med. Syst. 32 (6) (2008) 481–488.

[56] C.L. Nikias, J.M. Mendel, Signal processing with higher-order spectra, IEEE Signal Process. Mag. 10 (3) (1993) 10–37.

[57] V. Chandran, S.L. Elgar, Pattern recognition using invariants defined from higher order spectra-one-dimensional inputs, IEEE Trans. Signal Process. 41 (1) (1993) 205–212.

[58] S. Dua et al., Wavelet-based energy features for glaucomatous image classification, Ieee Trans. Inform. Technol. Biomed. 16 (1) (2012) 80–87.

[59] D. Giri et al., Automated diagnosis of coronary artery disease affected patients using LDA, PCA, ICA and discrete wavelet transform, Knowl.-Based Syst. 37 (2013) 274–282.

[60] R.M. Haralick, K. Shanmugam, Textural features for image classification, IEEE Trans. Syst., Man, Cybern. 6 (1973) 610–621.

[61] M.-K. Hu, Visual pattern recognition by moment invariants, IRE Trans. Inform. Theory 8 (2) (1962) 179–187.

[62] T. Ojala, M. Pietikainen, T. Maenpaa, Multiresolution gray-scale and rotation invariant texture classification with local binary patterns, IEEE Trans. Pattern Anal. Mach. Intell. 24 (7) (2002) 971–987.

[63] K.I. Laws, Rapid texture identification, in: SPIE Conference Series, vol. 238, 1980, pp. 376–380.

[64] A.P. Singh, B. Singh, Texture features extraction in mammograms using non-shannon entropies, in: Machine Learning and Systems Engineering, Springer, 2010, pp. 341–351.

[65] A.P.S. Pharwaha, B. Singh, Shannon and non-shannon measures of entropy for statistical texture feature extraction in digitized mammograms, in: proceedings of the World Congress on Engineering and Computer Science, 2009.

[66] Karmeshu, Entropy Measures, Maximum Entropy Principle and Emerging Applications, Springer Science & Business Media, 2003.

[67] V.P. Singh, Entropy Theory and Its Application in Environmental and Water Engineering, John Wiley & Sons, 2013.

[68] Q. Hu, D. Yu, Entropies of fuzzy indiscernibility relation and its operations, Int. J. Uncertainty, Fuzziness Knowledge-based Syst. 12 (05) (2004) 575–589.

[69] W.L. Hung, M.S. Yang, Fuzzy entropy on intuitionistic fuzzy sets, Int. J. Intell. Syst. 21 (4) (2006) 443–451.

[70] G.A. Darbellay, I. Vajda, Entropy expressions for multivariate continuous distributions, IEEE Trans. Inf. Theory 46 (2) (2000) 709–712.

[71] M. O'Mahony, Sensory Evaluation of Food: Statistical Methods and Procedures, CRC Press, 1986.

[72] R.A. Fisher, XV.—The correlation between relatives on the supposition of Mendelian inheritance, Earth Environ. Sci. Trans. Roy. Soc. Edinburgh 52 (2) (1919) 399–433.

[73] C. Cortes, V. Vapnik, Support-vector networks, Mach. Learn. 20 (3) (1995) 273–297.

[74] B.E. Boser, I.M. Guyon, V.N. Vapnik, A training algorithm for optimal margin classifiers, Proceedings of the Fifth Annual Workshop on Computational Learning Theory, ACM, 1992.

[75] F. Mosteller, A k-sample slippage test for an extreme population, in: Selected Papers of Frederick Mosteller, Springer, 2006, pp. 101–109.

[76] M. Bharara, J. Schoess, D.G. Armstrong, Coming events cast their shadows before: detecting inflammation in the acute diabetic foot and the foot in remission, Diabetes/Metabolism Res. Rev. 28 (S1) (2012) 15–20.

[77] O. Faust et al., Application of infrared thermography in computer aided diagnosis, Infrared Phys. Technol. 66 (2014) 160–175.

[78] U.R. Acharya et al., Automated characterization of fatty liver disease and cirrhosis using curvelet transform and entropy features extracted from ultrasound images, Comput. Biol. Med. 79 (2016) 250–258.

[79] M. Etehadtavakol, E.Y.K. Ng, Assessment of foot complications in diabetic patients using thermography: a review, in: Application of Infrared to Biomedical Sciences, Springer, 2017, pp. 33–43.

[80] J.H. Tan et al., Automated segmentation of exudates, haemorrhages, microaneurysms using single convolutional neural network, Inf. Sci. 420 (2017) 66–76.

[81] J.H. Tan et al., Segmentation of optic disc, fovea and retinal vasculature using a single convolutional neural network, J. Comput. Sci. 20 (2017) 70–79.